

Loop Makeup Identification Via Single Ended Testing: Beyond Mere Loop Qualification

Stefano Galli, *Member, IEEE*, and David L. Waring, *Senior Member, IEEE*

Abstract—Digital subscriber lines (DSLs) offer carriers the possibility of exploiting the existing loop plant to deliver high-speed data and voice services. However, before deploying DSL, local loops must be tested in order to see whether they can support service, and at what level. In fact, there are many impairments that could disqualify a loop for supporting DSL services: load coils, excessive loop length, bridged taps, and wideband noise. Single-ended automatic qualification is essential for achieving low-cost deployment of DSL, since it allows loops to be qualified in bulk and does not involve any human intervention at the customer's location. An even more ambitious challenge is to fully characterize a loop, i.e., to identify its loop makeup. If it is feasible to perform loop makeup identification via single-ended measurements with sufficient accuracy, then operators will benefit substantially because, besides qualifying a loop for DSL service, this capability will allow the updating of telephone company loop-records. These records can in turn be accessed to support engineering, provisioning and maintenance operations. Despite its potential importance, the possibility of achieving loop makeup identification via single-ended measurements is not widely addressed in the current literature. In the present contribution and in a companion paper to be submitted, the feasibility of loop makeup identification via single-ended measurements is presented.

Index Terms—Digital subscriber lines, time domain reflectometry techniques, twisted-pair modeling.

I. INTRODUCTION

THE UNSCREENED multipair cables in the existing subscriber loop network constitute the main access connection of telephone users to the telephone network. Recently, the demand for new services such as data, image, and video has tremendously increased, and telephone companies have planned to deliver broadband services via fiber optic local loops. However, the deployment of fiber optic cables in the access plant will evolve over many years. In the meantime, it is extremely important to fully exploit the existing copper cable plant. Digital subscriber line (DSL) technology was developed to exploit the embedded copper plant. Nowadays, there are many different DSLs: ISDN basic access, high bit-rate digital subscriber lines (HDSL), asymmetrical digital subscriber lines (ADSL) and very high rate digital subscriber lines (VDSL).

These services may not always be available to customers, depending on the makeup of the copper lines. In fact, the cable length and the presence of load coils and bridged taps may deeply affect the performance of DSL services. These technologies are engineered to operate over a class of subscriber loops,

such as nonloaded loops, or carrier serving area (CSA) loops. Today, the need to be able to “qualify” a loop for provision of one of these technologies is becoming critical, as the technologies emerge and deployment begins. The ability to easily and accurately qualify loops will allow telephone companies to offer a whole range of new services; converse problems and high expenses associated with qualifying loops can potentially inhibit deployment and/or lower or forego associated new revenues.

There are essentially three ways of carrying out a loop pre-qualification test: loop-record examination, single ended measurements, and double ended measurements.

Loop records historically were kept on paper, called “plats,” and more recently are manually entered into a computer database. However, even when entered into a database there are still problems associated with keeping the records accurate and up to date. A preliminary survey performed by Telcordia Technologies has determined that a significant percentage of existing loops have incomplete records and, moreover, the quality of the information kept in completed records may not always be reliable and up to date.

Double-ended measurements allow us to easily estimate the impulse response of a loop by using properly designed training sequences. However, this involves either the presence of a test device at the far end of the loop, e.g., a Smart Jack, or dispatching a technician to the subscriber's location (SL) to install a modem that communicates with the reference modem in the central office (CO).

Single-ended tests require that the test equipment be at the CO only and, therefore, are less time consuming and expensive than double-ended tests since no technician dispatching is required. On the other hand, single-ended testing is more demanding of the noise level at the receiver since the test signals have to propagate a complete round trip of the loop. The feature that allows efficient single-ended testing is the possibility of gaining metallic test access to the customer's line. Virtually all telephony equipment has *full-splitting metallic access* and is connected to a *metallic test bus* which terminates on a narrowband test-head (e.g., mechanized loop testing, or MLT, developed by the Bell System) for performing voice band tests in support of POTS service. By this means, a given subscriber loop can be taken out of service and routed, metallurgically, to a centralized test head where single-ended measurements can be made on the customer's loop. Currently, these techniques are useful for voice band services and were not intended for and do not address the problems associated with broadband services.

There are a number of solutions today that achieve loop qualification via single-ended testing. There are solutions based on the measurements of insertion losses or current imbalances. It

Manuscript received March 27, 2001; revised December 4, 2001.

The authors are with Telcordia Technologies, Inc., Morristown, NJ 07960 USA (e-mail: sgalli@telcordia.com; dlw@research.telcordia.com).

Publisher Item Identifier S 0733-8716(02)05366-0.

is often claimed that these solutions have the capability of detecting the presence and location of bridged taps. But, if multiple bridged taps are present, it may be difficult or impossible to exactly locate all of them. What can be induced is only the cumulative effects of all the bridged taps. An ideal (and more ambitious) solution would be capable of determining the exact *makeup* (topology) of the loop, i.e., the number of loop sections, the gauge kind of all the sections, and the location of gauge changes and bridged taps. Precise information on the topology of the loop implies loop qualification for DSL services: it allows us to determine accurately the frequency transfer function of the loop and, therefore, the possibility of determining the type and quality of service (QoS) that the line can support.

Current DSL qualification techniques do not have the possibility of precisely determining the QoS of a line, for example in terms of actual bit rate that can be supported. Rather, they often provide a simple binary answer to the question of loop qualification. The loop makeup can be effectively used to calculate the exact bit rate that a specific line can support. An even more precise assessment of the quality of service that a specific line can support can be made if additionally precise information on the crosstalk can be obtained, so that the usual pessimistic assumptions of worst-case crosstalk can be avoided. For this purpose, crosstalk identification techniques have been recently proposed in the literature [10], [11]. These techniques could be effectively combined with loop identification techniques to provide reliable, precise and nonbinary answers to the problem of DSL provisioning [9] (for example, by using calculations such as those in the DSL Spectral Compatibility Computer on the web page in [8]).

Information on the topology of the loop is of paramount importance for another reason, that transcends loop qualification itself. In particular, it can help telephone companies in updating and correcting their loop plant records. Moreover, these records can in turn be accessed to support engineering, provisioning and maintenance operations. For example, if a load coil is detected on the loop, the operator may decide to take it out so that the loop may then support DSL services. From this point of view, the feasibility of accurate loop makeup identification would have greater value than simple DSL qualification. However, despite its importance, the possibility of achieving loop makeup identification via single-ended measurements is not widely addressed in the current literature. In this paper, the feasibility of loop makeup identification via single-ended measurements presented.

The underlying physical phenomenon that allows estimation of the loop makeup is that gauge changes, bridged taps and the end of a loop represent a change in the characteristic impedance (a *discontinuity*) along the loop. When a signal is injected into a transmission line, a reflected and a transmitted wave are generated in correspondence to a change of the characteristic impedance. The part of the signal that is reflected back, the *echo*, contains all the information we need to detect the kind of discontinuity that caused it. Therefore, the analysis of all the echoes generated by probing a loop with a pulse, e.g., via time domain reflectometry (TDR) techniques, should allow us to induce the loop topology. However, there are two serious problems that do not allow for a straightforward application of conventional TDR techniques.

The first problem is due to the fact that conventional metallic TDRs are not capable of detecting all echoes. In fact, conventional metallic TDRs cannot detect gauge changes and, moreover, have a serious range limitation that prevents them from detecting echoes further than some number of kilofeet (kft) from the CO. This limitation is due to the presence of a slowly decaying signal, caused by the distributed RLC nature of the loop, that overlaps with and masks the echoes generated by impedance changes. The slowly decaying signal may be neglected when dealing with strong echoes, i.e., those generated by close discontinuities, but becomes manifest when weak echoes, i.e., those caused by gauge changes or far discontinuities, are considered. To the best of the authors' knowledge, the presence of this slowly decaying signal has not been reported in previous literature and has never been compensated for in today's TDRs. On the basis of the theoretical model developed here, it will be shown how to enhance the capabilities of a conventional metallic TDR in order to be able to detect gauge changes, as well as dramatically extending its range.

The second problem is that the available observations consist of an unknown number of echoes, some overlapping, some not, some spurious, some not, that exhibit unknown amplitude, unknown time of arrival, and unknown shape. The resolution of such echoes via a single sensor (and not an array) is very complicated and has seldom been addressed in the scientific literature. In fact, to the authors' best knowledge, there are only two contributions that address this problem [5], [6].

In the present paper, we give a mathematical model for the observations and propose a technique for solving the first problem. A possible solution to the second problem is described in a companion paper [7].

This paper is organized as follows. The major discontinuities along a telephone line that must be detected for achieving loop makeup identification are analyzed in Section II. The unavoidable presence of spurious echoes is addressed in Section III, where spurious echoes are also modeled and fully characterized. In Section IV, a mathematical model for the echoes is given and partially validated through lab measurements. The extension of the previous model to the case of weak echoes is addressed in Section V, and experimentally validated in Section VI. Finally, conclusive remarks are drawn in Section VII.

II. KINDS OF MEDIUM DISCONTINUITIES

The characteristics that must be estimated in order to identify properly the loop makeup are gauge changes, bridged taps, and the lengths of each loop section. Gauge changes, bridged taps, and the end of a loop constitute a change of impedance along the line. When a signal $s(t)$ is injected into a transmission-line, the signal undergoes distortion according to the physical characteristics of the medium. This distortion can be modeled as a filtering effect, where the filter is given by the transfer function of the section of cable on which the signal is traveling. Using the well-known ABCD coefficients notation, the transfer function of a loop can be expressed as follows:

$$H_f(f) = \frac{Z_L}{AZ_L + B + CZ_S Z_L + DZ_S} \quad (1)$$

where Z_S and Z_L are the source and load impedances, respectively. For more details on the ABCD notation see [2, Ch. 3]. For an interesting property of the transfer function of a loop only recently reported see [3].

Whenever the traveling signal encounters a change of impedance, part of this signal (echo) is reflected back. An index of the “amount” of signal that is reflected back is given by the *reflection coefficient* $\rho(f)$ (see [1, Ch. 2])

$$\rho(f) = \frac{Z_a - Z_b}{Z_a + Z_b} \quad (2)$$

where Z_a and Z_b are the characteristic impedances after and before the discontinuity, respectively. The reflection coefficient $\rho(f)$ is defined as the ratio of the reflected wave to the incident wave and, usually, it is a complex function of frequency. It can be viewed as a sort of filter that ties the incident signal (the probing signal) to the reflected signal (the echo).

When a signal $s(t)$ encounters a change of characteristic impedance, part of the incident wave is reflected back along the line and filtered by $\rho(f)$ and part will travel on to the next loop section. The part of the signal that travels on to the next loop section will be modified by the so-called voltage *transmission coefficient* $\tau(f)$ defined as follows [4, Sec. 2.2]:

$$\tau(f) = 1 + \rho(f) = \frac{2Z_a}{Z_a + Z_b}. \quad (3)$$

The transmission coefficient is defined as the ratio of the voltage that is refracted by the junction to the incident voltage. This coefficient is frequency dependent and introduces a filtering effect on the refracted signal.

From the foregoing, the shape of an echo depends on the kind of discontinuity [through the reflection coefficient $\rho(f)$] and on the loop sections preceding the discontinuity that generated the echo [through the transfer function $H(f)$, and the transmission coefficient $\tau(f)$]. The reflection coefficient $\rho(f)$ is different for each discontinuity and puts a sort of “discontinuity signature” on the echo. At the end of Section VI, we will show that different discontinuities will yield echoes of different shape, thus confirming the possibility of identifying the type of a discontinuity on the basis of the shape of the echo that was generated.

In the following sections, the filtering effect of each kind of discontinuity will be analyzed in terms of the characteristics of the reflection and transmission coefficients. Plots of the magnitude of $\rho(f)$ will be presented. These plots are generated on the basis of an accurate model of the primary characteristics of twisted pairs. On the basis of these primary characteristics, it is possible to compute the characteristic impedance and the propagation constant of twisted-pairs of any gauge and length. In so doing, the ABCD coefficients of a loop section can be easily derived. This accurate model has been derived on the basis of theoretical analysis as well as on the basis of a large measurement campaign performed in our labs.

A. Change of Gauge-Type

Telephone cables are usually deployed following the *regular gauging* design rules, i.e., cables near the CO have a thinner diameter while cables near the SL have a thicker diameter. Thinner cables have higher characteristic impedance than

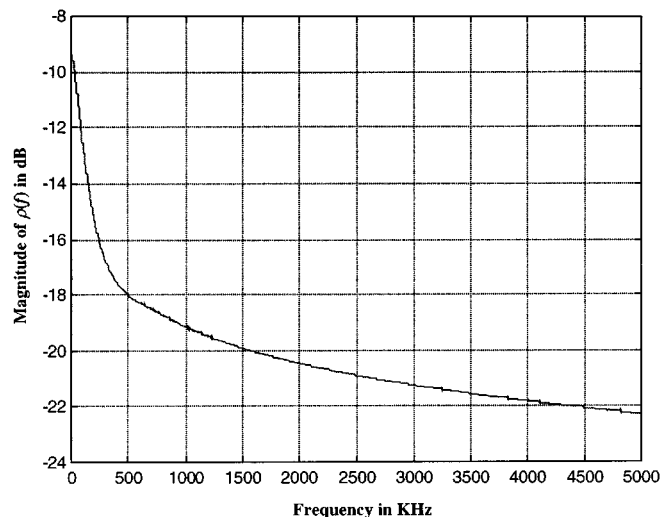


Fig. 1. Behavior of the magnitude of the reflection coefficient $\rho(f)$ in (2) for the case of a gauge change from an AWG26 cable to an AWG24 one.

thicker ones, so a signal that encounters this discontinuity passes from a medium with higher impedance to a medium with lower impedance.

In Fig. 1, the magnitude of the reflection coefficient $\rho(f)$ versus frequency is plotted for a gauge change from AWG 26 to AWG 24. The magnitude becomes highly attenuated within a few hundred kilohertz. In general, when a signal travels on a loop and passes from a section with higher characteristic impedance to a section with a lower one, the echo will always be negative. And vice versa; when a signal travels on a loop and passes from a section with lower characteristic impedance to a section with a higher one, the echo will always be positive.

From Fig. 1, it can also be verified that the magnitude of the transmission coefficient $\tau(f) = 1 + \rho(f)$ for a gauge change from AWG 26 to AWG 24 exhibits a nearly flat response of 0 dB over the entire bandwidth. Therefore, there will be a negligible change in the refracted signal that travels on to the next loop section.

B. End of the Loop

Let us consider a loop terminated by an on-hook telephone. The input impedance of an on-hook telephone is generally very high when compared to the impedance characteristics of the cable. We have measured the input impedance of a sample of nine different types of telephones, including a cordless telephone and an old rotary telephone, in the frequency range from 10 to 1.5 MHz. Results are summarized in Fig. 2. On the basis of these results, we can state that the assumption that the telephone at the customer’s premises exhibits a high input impedance is a reasonable one, although it may not always be true.¹ We will

¹There may be other reasons for which this assumption may not be true: leaky or shorted primary protection gas tubes or carbon blocks; improper wiring at the subscriber end that may have either tip or ring grounded; off-hook or malfunctioning telephone at the subscriber end. However, current voice band loop testing equipment such as MLT can effectively identify these “pathological” situations. In our approach, passing voice band loop testing is a prerequisite for broadband loop testing. After all, if a connection does not work for voice, it is very likely that it will also not work for DSL.

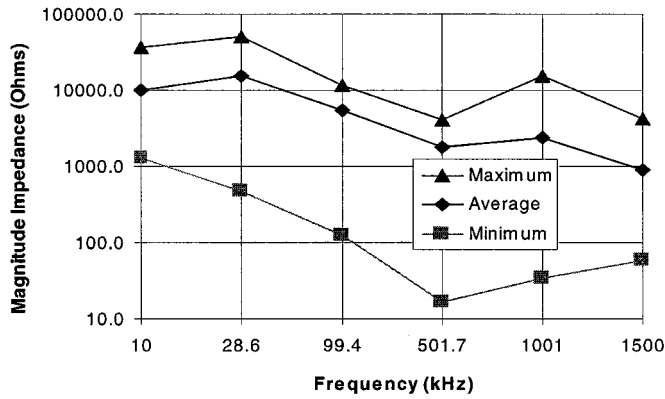


Fig. 2. Measured on-hook impedances of nine telephones at selected frequencies.

here assume that an on-hook telephone can be well approximated by an open circuit (see also [1]). In this case, the reflection coefficient boils down to the following expression (Z_a is an infinite impedance):

$$\rho(f) = \lim_{Z_a \rightarrow \infty} \frac{Z_a - Z_b}{Z_a + Z_b} = 1.$$

Therefore, an infinite impedance will simply send back the signal with no attenuation and no sign change. In this case, the only distortion will be caused by the transfer function and the transmission coefficients of the loop sections on which the signal has traveled.

C. Bridged Taps

A bridged tap occurs whenever a branching connection is spliced onto the cable, a situation that is very common in the outside plant. The end of the branch is usually open. In the case of a bridged tap, the traveling wave sees the parallel of the impedance of the bridged-tap and of the following loop-section. This means that the echo generated at the junction will be negative, since the signal passes from a medium with higher characteristic impedance to a medium with lower characteristic impedance.

The junction will also generate two refracted waves: one wave will travel along the bridged tap and the other one will travel in the next loop section. The end of a bridged tap is normally an open circuit, so in this case the traveling wave will be totally reflected since $\rho(f) = 1$ for an open circuit, and the polarity of the echo will be positive. This means that if there is a bridged tap, the CO will observe the subsequent arrival of a negative echo followed by a positive echo.

If the loop section preceding the junction, the bridged tap and the section following the junction are all of the same kind of gauge and if these sections are sufficiently long, the reflection coefficient boils down to the following expression (Z_a is the parallel of two equal characteristic impedances $Z_b = Z$):

$$\rho(f) = \frac{Z_a - Z_b}{Z_a + Z_b} = \frac{Z/2 - Z}{Z/2 + Z} = -\frac{1}{3}.$$

So, in this simple case the echo will not be distorted by the discontinuity but will only be attenuated and reversed in sign.

In Fig. 3(a) the magnitude of $\rho(f)$ versus frequency is plotted for the configuration in Fig. 3(b). The attenuation is lower than

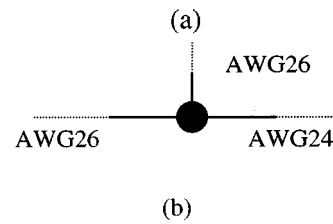
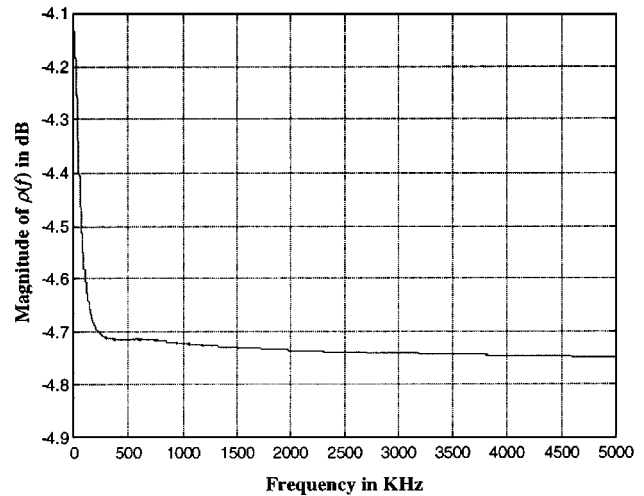


Fig. 3. (a) Behavior of the magnitude of the reflection coefficient $\rho(f)$ in (2) for the case of the bridged tap showed in (b).

in the case of a gauge change and, after few hundred kilohertz, the attenuation is approximately constant and asymptotically reaches the value of $10 * \log_{10}(1/3)$.

In contrast to the gauge change case, the value of the transmission coefficient $\tau(f)$ is no longer negligible. In fact, when $\rho(f) = -1/3$ it follows that $\tau(f) = 2/3$. The absolute value of $\tau(f)$ may be considered flat over the whole bandwidth with an attenuation of $10 * \log_{10}(2/3)$.

III. SPURIOUS ECHOES

The presence of spurious echoes is due to the fact that each discontinuity generates both a reflected and a refracted signal, so that a part of the signal travels back and forth on the line, bouncing between discontinuities, before it arrives at the CO. In the following, we define as *real echoes* the echoes pertaining to initial encounters with discontinuities, whereas we will define as *spurious echoes* all the echoes caused by successive reflections. Obviously, the more the spurious echo travels on the line the more attenuation it will suffer upon arrival at the CO. However, the effect of these spurious echoes must not be neglected since spurious echoes generated at a discontinuity may sometimes be even stronger than the real echoes generated by the following discontinuities.

The necessity of separating echoes in two categories (“real” and “spurious”) may not be evident now that we are dealing with modeling issues, but it becomes important when loop identification is attempted [7]. In fact, any identification algorithm must be able to discriminate between *real* echoes (the echoes that indicate the actual presence of a *real* discontinuity) and *spurious* echoes (the re-reflected and artificial echoes that do not indicate the presence of a discontinuity). Only real echoes should

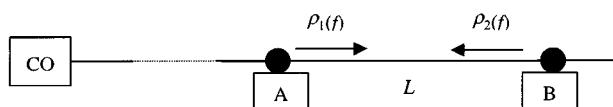


Fig. 4. Loop configuration considered for the determination of the spurious echoes generated in correspondence of a gauge change.

be analyzed by the identification algorithm and attributed to the corresponding discontinuity that generated it, whereas spurious echoes should be discarded as false echoes.

In the following sections, we will analyze the main spurious echoes generated on a loop and we will also give some simulation results. We will find the echo path and the reflection coefficient of all the possible spurious echoes. The determination of the echo path is important because it allows us to build the transfer function $H(f)$. The reflection coefficient is also an important quantity for the description of spurious echoes and will consist of several terms, each of which will account for the consecutive bouncing of the echoes.

A. The Spurious Echoes: Gauge Changes

Let us consider the situation depicted in Fig. 4, where a gauge change (labeled A) is followed by a discontinuity (labeled B). The second discontinuity in B can be any discontinuity since its behavior is entirely described by the reflection coefficient $\rho_2(f)$. When the signal arrives at A, an echo is generated and goes back to the CO; this is a real echo and pertains to the discontinuity at A. The refracted part of the signal travels on and arrives at B, where another echo is generated in accordance with the reflection coefficient $\rho_2(f)$. When this second echo arrives back at A, part of it will be refracted and will constitute the real echo pertaining to the discontinuity B and part will be reflected back toward B in accordance with the reflection coefficient $\rho_1(f)$. Theoretically, the part of signal going back toward B can bounce an infinite number of times between A and B, and, at each bouncing, a refracted and a reflected wave will be generated. For this reason, an infinite number of spurious echoes will be received in the CO.

It is possible to prove that the echo path and the reflection coefficient pertaining to the i th spurious echo generated by two consecutive gauge changes are the following ($i > 0$):

$$\begin{aligned} \text{Path} &= \text{Path from CO to A} + 2(i+1)L \\ &\quad + \text{Path from A to CO} \\ \rho(f) &= [\rho_1(f)]^i [\rho_2(f)]^{i+1}. \end{aligned}$$

B. The Spurious Echoes: Bridged Taps

Let us now consider the situation depicted in Fig. 5, where a bridged tap (labeled A) and a discontinuity (labeled C) are present in the loop. The discontinuity in C can be either a gauge change or another bridged tap, and its behavior is entirely described by the reflection coefficient $\rho_3(f)$. When the signal arrives in A, an echo is generated and goes back to the CO; this is a real echo and pertains to the discontinuity at A. After encountering A, part of the signal travels on and arrives at B and part travels on arriving at C. In this case, there are three kinds of spurious echoes:

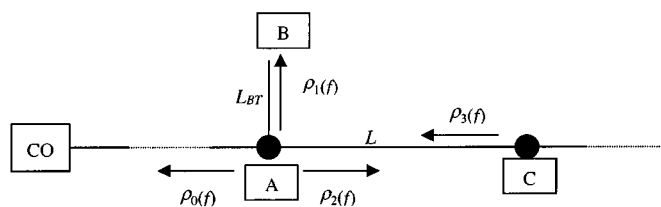


Fig. 5. Loop configuration for the determination of the spurious echoes generated in correspondence of a bridged tap.

- 1) the spurious echoes that bounce between A and B and go back to the CO;
- 2) the spurious echoes that bounce between A and B, travel on toward C and go back to the CO;
- 3) the spurious echoes that bounce between A and C and go back to the CO.

The echo paths and the reflection coefficients pertaining to the above mentioned types of echoes are listed in the following.

Type 1 ($i > 0$):

$$\begin{aligned} \text{Path} &= \text{Path from CO to A} + 2(i+1)L_{BT} \\ &\quad + \text{Path from A to CO} \\ \rho(f) &= [1 + \rho_0(f)][1 + \rho_1(f)][\rho_1(f)]^i. \end{aligned}$$

Type 2 ($i, j > 0$):

$$\begin{aligned} \text{Path} &= \text{Path from CO to A} + 2iL_{BT} + 2jL \\ &\quad + \text{Path from A to CO} \\ \rho(f) &= [1 + \rho_0(f)][1 + \rho_1(f)][1 + \rho_2(f)] \\ &\quad \cdot [\rho_1(f)]^{i-1} [\rho_2(f)]^{j-1} [\rho_3(f)]^j. \end{aligned}$$

Type 3 ($i > 0$):

$$\begin{aligned} \text{Path} &= \text{Path from CO to A} + 2(i+1)L \\ &\quad + \text{Path from A to CO} \\ \rho(f) &= [1 + \rho_0(f)][1 + \rho_2(f)][\rho_2(f)]^i [\rho_3(f)]^{i+1}. \end{aligned}$$

In the case that the consecutive discontinuities consist of the same kind of gauge, the above reflection coefficients boil down to the following expressions:

$$\begin{aligned} \text{Case 1: } \rho(f) &= \frac{4}{9} \left(-\frac{1}{3}\right)^i \\ \text{Case 2: } \rho(f) &= \frac{8}{27} \left(-\frac{1}{3}\right)^{i+j-2} [\rho_3(f)]^j \\ \text{Case 3: } \rho(f) &= \frac{4}{9} \left(-\frac{1}{3}\right)^i [\rho_3(f)]^{i+1}. \end{aligned}$$

The spurious echoes produced in correspondence to a bridged tap are stronger than those produced by a gauge change. The spurious echoes are still smaller than the real ones but much stronger than for the gauge change case and can definitely change the peak sequence, causing the appearance of false peaks. If the bridged tap is longer, the spurious echoes are weaker but so are the real echoes.

IV. A FIRST MATHEMATICAL MODEL FOR THE ECHOES AND ITS PARTIAL EXPERIMENTAL VALIDATION

As discussed in Sections II and III, every discontinuity generates echoes. The shape of these echoes depends on the transfer function of the echo path and on the reflection coefficients of the

actual discontinuity as well as on the transmission coefficient of all the preceding discontinuities.

In the following sections, we will present a mathematical model for the echoes and experimental results that will *partially* validate the model. In fact, the model developed here holds only for the case of short loops (up to few kft). The inability of this model to describe the behavior of echoes on long loops is due to the distributed RLC nature of the loop, and its manifestation through the presence of a slowly decaying signal. As will be shown in Section V, it is possible to model and counterbalance the slowly decaying signal so that a new and complete model of the echo response of a loop can be derived.

A. Mathematical Model

On the basis of the previous considerations, N discontinuities present in the loop will generate N real echoes whose shape will depend both on the kind of discontinuity and on the loop sections on which the echo has traveled. Moreover, a theoretically infinite number of spurious echoes will be also generated. Therefore, the observed signal $r(t)$ can be expressed as the following:

$$r(t) = \sum_{i=1}^N e_r^{(i)}(t - \xi_i) + \sum_{i=N+1}^{\infty} e_s^{(i)}(t - \xi_i) \quad (4)$$

where $e_r^{(i)}(t)$ ($i = 1, 2, \dots, N$) is the i th *real echo* generated by the i th discontinuity, $e_s^{(i)}(t)$ ($i = N + 1, N + 2, \dots$) is the i th *spurious echo*, and ξ_i is the time of arrival of the i th echo at the CO. The real echo $e_r^{(i)}(t)$ can be expressed as the following:

$$e_r^{(i)}(t) = s(t) * h_{r-ep}^{(i)}(t) \quad (5)$$

where $h_{r-ep}^{(i)}(t)$ is the i th (real) echo path impulse response. In the frequency domain, the corresponding (real) echo path transfer function $E_{r-ep}^{(i)}(f)$ can be expressed as

$$\begin{aligned} E_{r-ep}^{(i)}(f) &\equiv F \left[h_{r-ep}^{(i)}(t) \right] \\ &= K \left(\tau^{(1)}, \tau^{(2)}, \dots, \tau^{(i-1)} \right) H^{(i)}(f) \rho^{(i)}(f) \end{aligned} \quad (6)$$

where $H^{(i)}(f)$ is the transfer function pertaining to the round trip path of the i th echo (from the CO to the discontinuity and back to the CO again); the frequency dependent term $K(\tau^{(1)}, \tau^{(2)}, \dots, \tau^{(i-1)})$ takes into account the transmission coefficients $\tau(f)$ pertaining to all discontinuities preceding the i th one; and $\rho^{(i)}(f)$ is the reflection coefficient of the i th discontinuity that generated the i th real echo.

Spurious echoes can be modeled in a similar fashion, since spurious echoes depend on the same quantities that real echoes depend on. In particular, we can write

$$\begin{aligned} e_s^{(i)}(t) &= s(t) * h_{s-ep}^{(i)}(t) \\ E_{s-ep}^{(i)}(f) &\equiv F \left[h_{s-ep}^{(i)}(t) \right] = H^{(i)}(f) \rho^{(i)}(f) \end{aligned}$$

where the expressions of the echo paths and the reflection coefficients are the ones given in Section III.

B. Partial Experimental Validation

A preliminary set of measurements was performed in our lab using common equipment available on the market. The output of

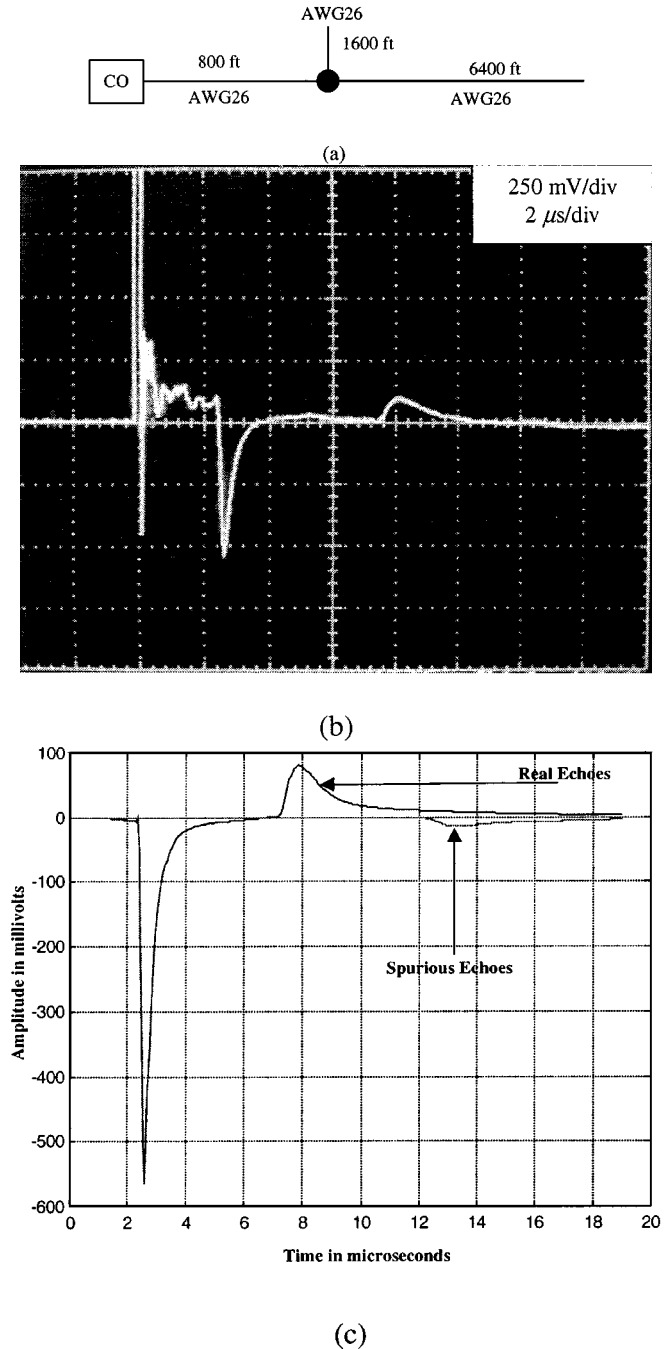


Fig. 6. Comparison of the measured echo (b) and the echo predicted by the analytical model (c) for the loop in (a). In (c), real echoes and spurious echoes are plotted separately. Only, the first 35 spurious echoes have been considered.

a pulse generator was a square wave of 5 Vs (on 50 ohms) with a width of 200 ns and a 5-ns rise and fall time. At the output of the pulse generator a balun provided a 50 ohms unbalanced to a 100 ohms balanced conversion² and, at the output of the balun, the loop under test. The oscilloscope was connected at the beginning of the loop in a differential way.

The experiment measured the echo generated by the bridged tap in Fig. 6(a) and (b) shows the output of the oscilloscope. The negative-positive sequence (as predicted in Section II-C) is

²The presence of the balun makes the amplitude of the wave actually injected into the loop equal to $5 \cdot \sqrt{2}$ Vs.

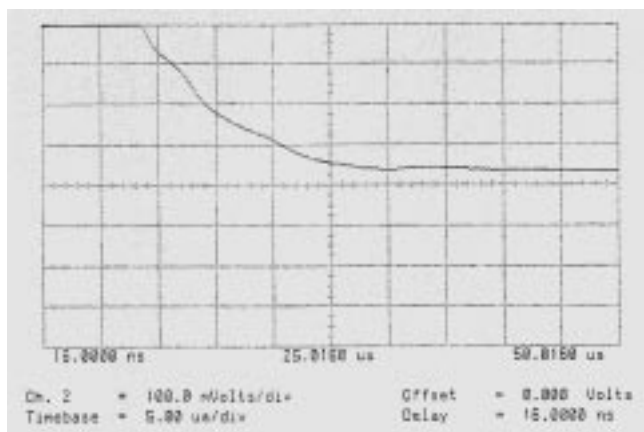


Fig. 7. Measured TDR trace for the loop with the following topology: 6 kft of AWG 26, a 1.5 kft bridged tap of AWG 24, 3 kft of AWG 22. Probing signal: 5 V (over 100 ohms) and 3 μ s square pulse.

clearly visible: the first negative echo has a peak of -558 mV and a width at half its peak of 380 ns, whereas the second positive echo has a peak of 89 mV and a width of 1.26 μ s. The echo predicted by the analytical model (4)–(6) is shown in Fig. 6(c). In this plot, the contribution of real and spurious echoes has been shown separately to show that spurious echoes may sometimes be appreciable.

Although the model would predict the generation of echoes by gauge changes, it was impossible to detect them experimentally. Moreover, when considering longer loops it was also impossible to detect the presence of echoes due to a bridged tap or to the end of a loop. In order to exclude the possibility that this was due to the inaccuracy of the equipment used in our experiments, we performed the same measurements using one of the most sensitive metallic TDRs available on the market. The results did not change at all. An example is given in Fig. 7, where a measured TDR trace is shown for the loop with the following topology: 6 kft of AWG 26, a 1.5-kft bridged tap of AWG 24, 3 kft of AWG 22. The model in Section IV-A would have predicted a negative/positive echo sequence. However, as can be seen in Fig. 7, no echo is visible in the TDR trace. Similarly, the TDR could not detect the echo due to a gauge change even though the model predicts its existence. In the following section, the reason for this behavior will be explained, and a new model that is valid on loops of any length will also be derived.

V. EXTENSION OF THE MODEL TO THE DETECTION OF VERY WEAK ECHOES

When measuring weak echoes such as those generated by far discontinuities or by gauge changes, the model given in Section IV falls short. This is due to the fact that the model in Section IV does not take into account the distributed RLC behavior of the loop. If the echo is very strong, this behavior may be neglected, whereas in the case of weak echoes, this approximation turns out to be too harsh.

Let us consider the circuit shown in Fig. 8(a), where the loop is represented by a two-port network (2PN). If we apply the Thevenin theorem to the circuit in Fig. 8(a), the part of the circuit highlighted in gray may be represented by a single

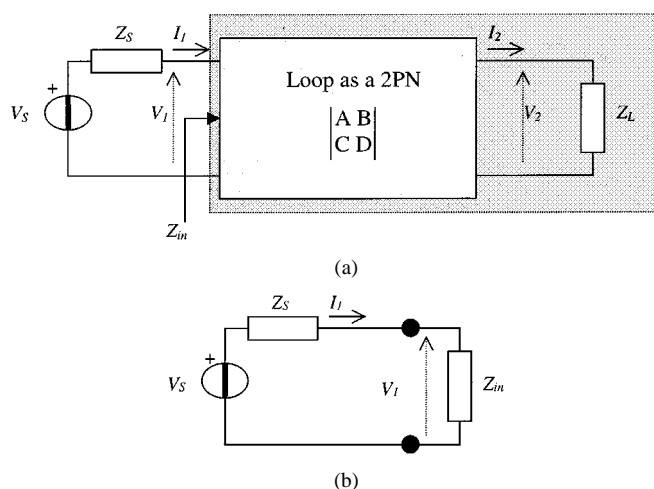


Fig. 8. (a) A two-port network with the signal source (generator V_S and its internal impedance Z_S) connected to the first port and the load impedance Z_L connected to second port. (b) The equivalent circuit of (a), after having applied the Thevenin theorem to the gray part of the circuit.

impedance equal to the input impedance of the 2PN (i.e., the input impedance of the loop) as shown in Fig. 8(b)

$$Z_{\text{in}}(f) = \frac{AZ_L + B}{CZ_L + D}. \quad (7)$$

The input impedance of the loop is a complex function of frequency and obviously depends on the termination of the loop, the load impedance Z_L . In the case of an unterminated loop (i.e., infinite load impedance), the relationship in (7) boils down to the following expression:

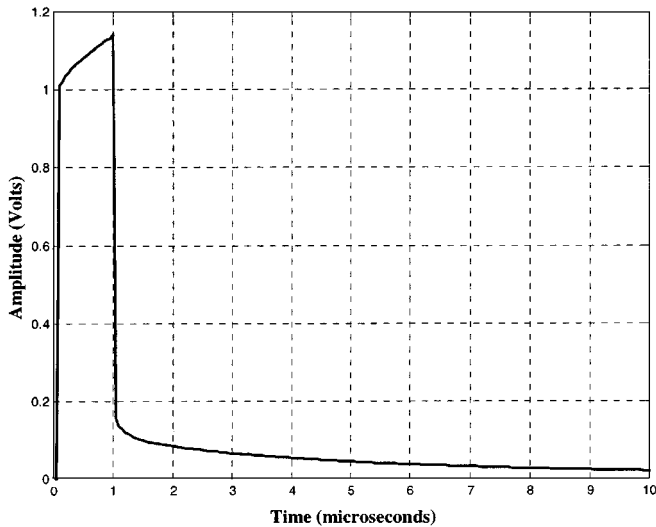
$$Z_{\text{in}}^{(\text{unterm})}(f) = \lim_{Z_L \rightarrow \infty} \frac{AZ_L + B}{CZ_L + D} = \frac{A}{C}. \quad (8)$$

The waveform actually entering the loop is V_1 [see Fig. 8(b)] and is tied to the source waveform V_S according to the following:

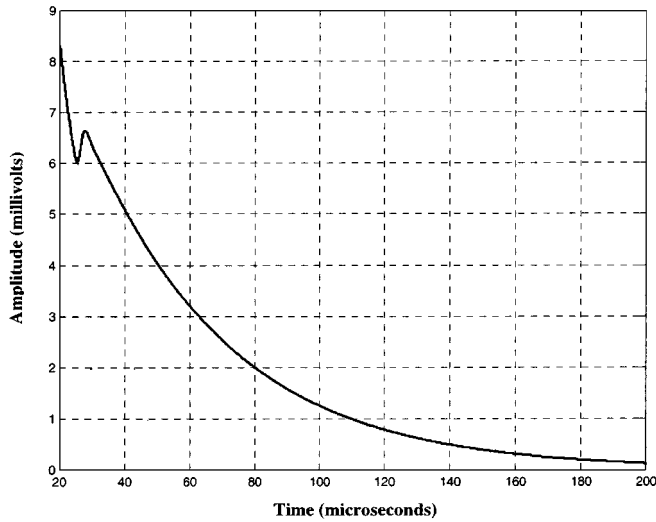
$$V_1(f) = \frac{Z_{\text{in}}}{Z_{\text{in}} + Z_S} V_S(f). \quad (9)$$

As an example, let us consider the case of an ideal square pulse of 1 μ s in width and 1 V (over 100 ohms) of amplitude injected into an unterminated, 8-kft long 26 AWG cable. The simulated behavior of V_1 versus time is plotted in Fig. 9. From Fig. 9(a) it can be seen that the actual waveform entering the loop is not a square waveform anymore. In particular, the signal does not go to zero at $t = 1$ μ s, but drops down to approximately 120 mV and then decays very slowly toward zero. Moreover, the positive echo due to the end of the loop is not visible. This phenomenon is negligible if the amplitude of the echoes is high, but has to be taken into account when dealing with very weak echoes. In particular, the observed signal decays slowly toward zero and the arriving echo overlaps with this slowly decaying signal. This can be seen in Fig. 9(b) where the waveform has been plotted from $t = 20$ μ s to $t = 200$ μ s. The little spike present at approximately 25 μ s represents the echo generated by the end of the loop and is superimposed on the decaying signal previously mentioned.

The echo overlapping the decaying signal is visible if it is sufficiently strong, has a sharp rise and if it is not too broad. For this reason it is difficult to detect echoes coming back from very



(a)



(b)

Fig. 9. (a) Voltage across an unterminated, 8 kft long, 26 AWG cable when the injected signal is a 1 V and 1 μ s square pulse. (b) Same as in (a), but the time axis goes from 20 to 200 μ s.

long loops since those echoes are very weak and broad (see, for example, the measured TDR trace shown in Fig. 7). It is worth pointing out that the presence of the decaying waveform is not due to the particular choice of the probing signal. In fact, even if a different probing signal were used, the received echoes would still be superimposed on a slowly decaying waveform since this is due to an intrinsic behavior of the loop.

Since the presence of this decaying signal is unavoidable, the only way to reduce its effects is to act on the received echoes. Fortunately, it is possible to compute analytically the expression of the slowly decaying waveform. In order to compute this expression, we have to consider that the signal injected into the loop “sees” a load equal to the characteristic impedance of the first section of the loop. This may not be evident in the models shown in Fig. 8 because those models describe the loop as a 2PN and neglect the fact that the loop is actually a transmission line and not a simple circuit with discrete lumped components. The input impedance of the loop that appears in (9) gives a *global* de-

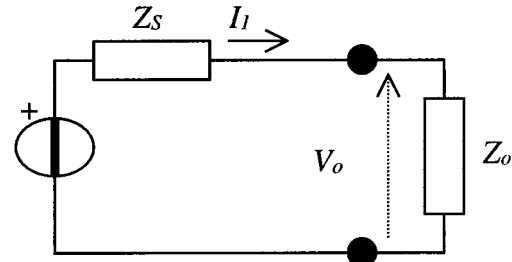


Fig. 10. The equivalent circuit of Fig. 8 used for the computation of the slowly decaying waveform superimposed to the echoes.

scription of the response of the *whole* loop to a probing signal, but if we want to take into account that the loop is actually a transmission line we have to consider that it is the first section of the loop that influences the characteristics of the signal entering the loop. In fact, the probing signal injected into the line propagates along the loop as if it were traveling along an infinitely long loop. Since the input impedance of an infinitely long loop is equal to its characteristic impedance, the correct model describing the voltage across the pairs at the moment the probing signal is injected into the loop is the one in Fig. 10, where Z_o is the characteristic impedance of the first loop section.

The model in Fig. 10 remains valid until the traveling wave encounters a discontinuity along the line, e.g., a gauge change, a bridged tap, an unterminated end, etc. The presence of a discontinuity along the line causes an abrupt change in the boundary conditions of the equation describing the traveling wave. Moreover, on the basis of causality arguments, the changes on the probing signal caused by discontinuities will always take place after these discontinuities are encountered and will not influence at all the shape of the traveling wave before they are encountered. Therefore, we can express the slowly decaying waveform in the following form:

$$V_o(f) = \frac{Z_o}{Z_o + Z_S} V_S(f). \quad (10)$$

Equation (10) is the *exact* expression of the slowly decaying waveform until the first discontinuity has been encountered and its effect (the echo) has arrived back at the beginning of the loop. The waveform in (10) can be calculated in two ways: it can be calculated on the basis of a model of the characteristic impedance of the twisted pair, or it can be experimentally measured by probing and infinitely (e.g., 30 kft) long loop.

As previously mentioned, the voltage $V_1(f)$ given in (9) is the waveform obtained when we consider the loop as a discrete lumped circuit (and, therefore, all the discontinuities along the loop are included) whereas the voltage $V_o(f)$ in (10) is the waveform obtained when we take into account the actual nature of the loop as a transmission line (and, therefore, only the presence of the first loop section). On the basis of the previous considerations, subtracting $V_o(f)$ from $V_1(f)$ should remove the slowly decaying waveform and allow us an easier detection of weak and broad echoes. Moreover, the difference $(V_1(f) - V_o(f))$ should also lead us to (approximately) the same results predicted by the model in Section IV-A that did not take into account the presence of the slowly decaying signal. So, the echo $V(f)$ predicted

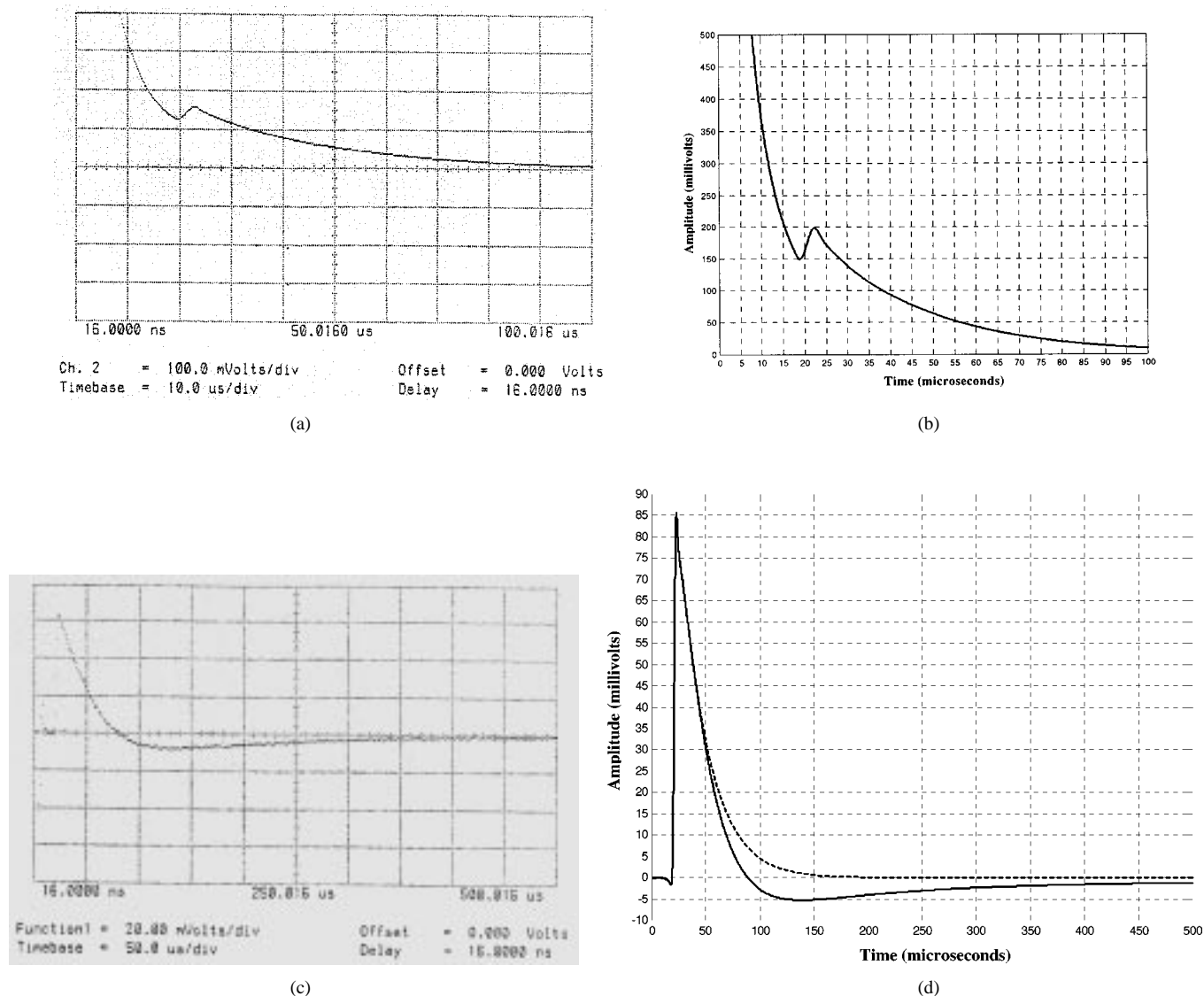


Fig. 11. *End of Loop*: Comparison of measurement results and simulation results for the unterminated, AWG 26, 6-kft-long loop. Probing signal: 5-V and 3- μ s-square pulse.

by the model in Section IV-A should be approximately given by the following expression:

$$\begin{aligned}
 V(f) &= V_1(f) - V_o(f) \\
 &= \left[\frac{Z_{in}}{Z_{in} + Z_S} - \frac{Z_o}{Z_o + Z_S} \right] V_S(f) \\
 &= \frac{(Z_{in} - Z_o)Z_S}{(Z_{in} + Z_S)(Z_o + Z_S)} V_S(f). \quad (11)
 \end{aligned}$$

The subtraction technique can be performed in two ways, depending on how the slowly decaying signal $v_o(t)$ is obtained. First, the loop under test is probed with signal $s(t)$ and the resulting waveform $v_1(t)$ is measured. The waveform $v_o(t)$ can be either computer generated on the basis of a model of the characteristic impedance of twisted-pair or it can be measured as the response to the probing signal $s(t)$ of a very long loop of the same gauge as the first loop section of the loop under test. Finally, $v_o(t)$ is subtracted from $v_1(t)$.

It is worth pointing out that, to the authors' best knowledge, the technique of subtracting the slowly decaying signal of (10) from the observation has never been used in commercial TDRs. These theoretical results have been confirmed by an experimental campaign performed in our labs. Some measurement results will be given in the following section.

VI. FINAL EXPERIMENTAL VALIDATION OF THE MODEL

The probing signal used in our experiments is a square pulse of 5 V_s (on 100 ohms) with a width of τ μ s and a 5 ns rise and fall time. The width τ of the pulse chosen for the measurement experiment will vary depending on the length of the loop.³ In particular, for every loop makeup we will show four figures:

- the scanned print-output of the oscilloscope for the echo observation process pertaining to the loop under test (i.e., including the slowly decaying signal);

³Wider pulses allow us to detect far discontinuities at the price of an increase in the broadness of the received echo and, in turn, a loss of resolution.

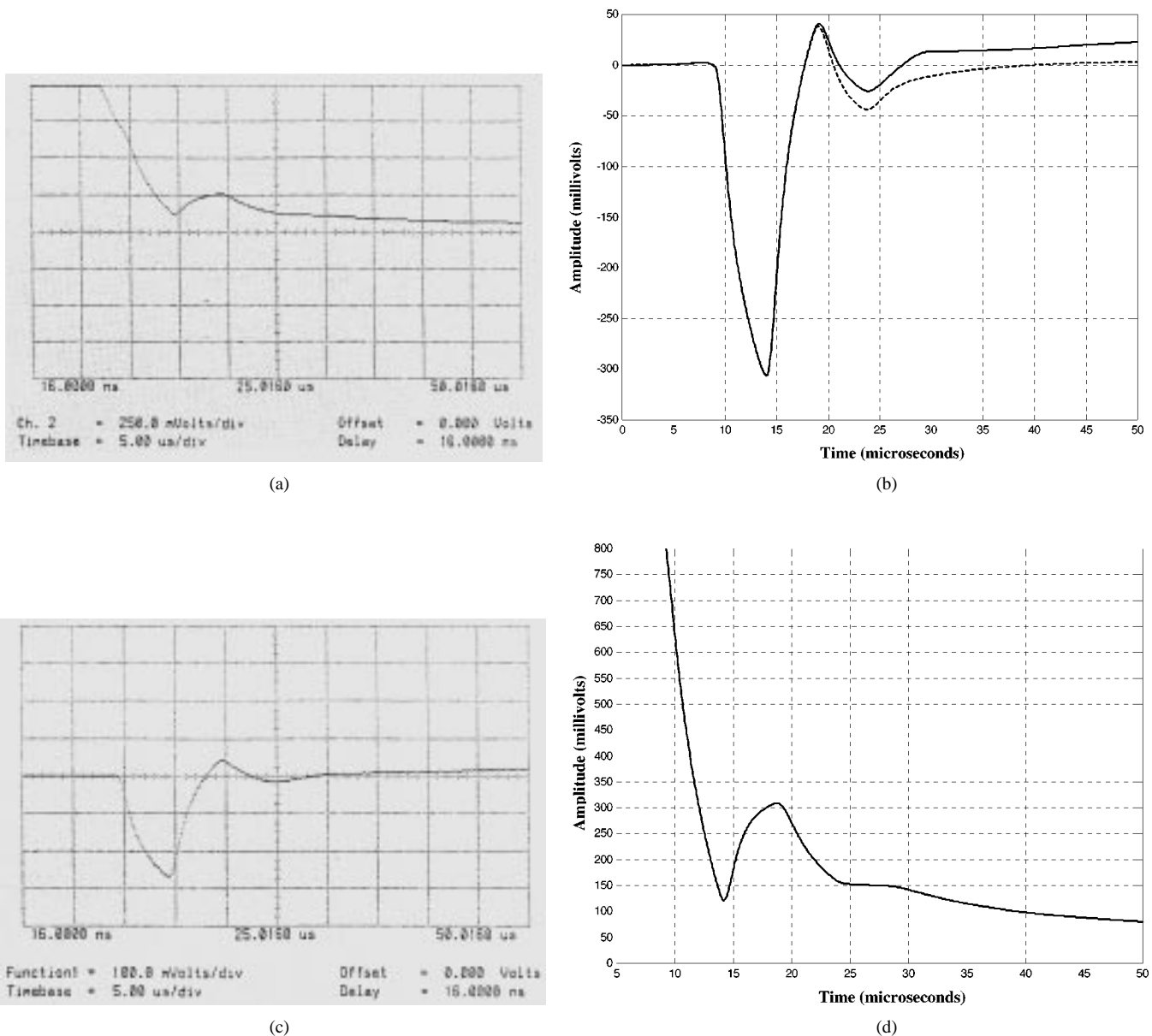


Fig. 12. *Bridged Tap*: Comparison of measurement results and simulation results for the following loop: 3 kft of AWG 26, a 1.5 kft bridged of AWG 24, 1.5 kft of AWG 26, a 1.5 kft bridged of AWG 24, and a final section of 6 kft and AWG 26. Probing signal: 5 V and 5 μ s square pulse.

- b) the simulation result using the model represented by (9);
- c) the scanned print-out of the oscilloscope representing the difference between the echo observation process and the slowly decaying signal;⁴
- d) a solid line representing the simulation result using the model represented by (11), and a dashed line representing the simulation result obtained on the basis of the model described by (4).

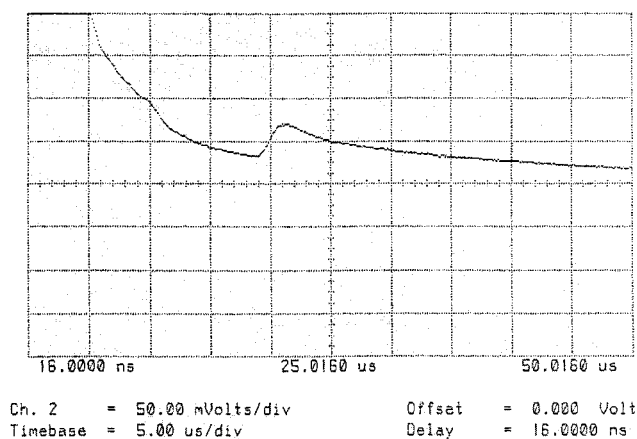
The validation of the developed models can be obtained comparing figures a) and b) for the model in (9), and comparing figures c) and the solid line in d) for the model represented

⁴The signal subtracted from the echo observation process was measured as the response to the probing signal of a very long cable (36 kft) of the same gauge as the first loop section of the loop under test. This ensures that the response of the long loop is the same response that would be given by a load equal to its characteristic impedance and this would well simulate the model in Fig. 10. The obtained signal was stored in the oscilloscope and, then, subtracted from the signal representing the response of the loop under test.

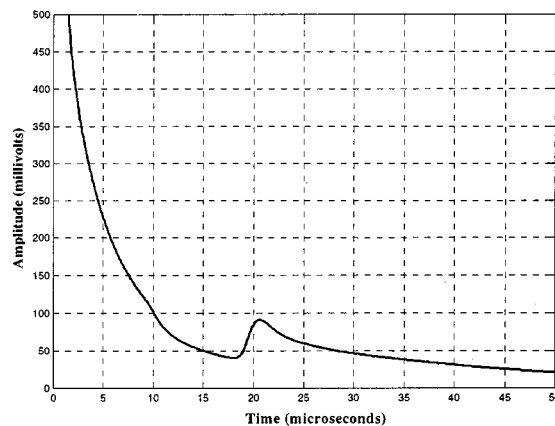
in (11). Finally, a comparison between the model developed in Section IV and the one developed in Section V can be made by comparing the two curves (solid and dashed) shown in figure d).

Among the several experiments we have performed, we present here three cases. The first loop under test is an unterminated 26-AWG 6-kft-long loop (see Fig. 11). The second loop has the following topology: 3 kft of AWG 26, a 1.5-kft bridged of AWG 24, 1.5 kft of AWG 26, a 1.5-kft bridged of AWG 24, and a final section of 6 kft and AWG 26 (see Fig. 12). The third loop under test consists of a 3-kft AWG 26 cable followed by 3 kft of a AWG 24 cable (see Fig. 13).

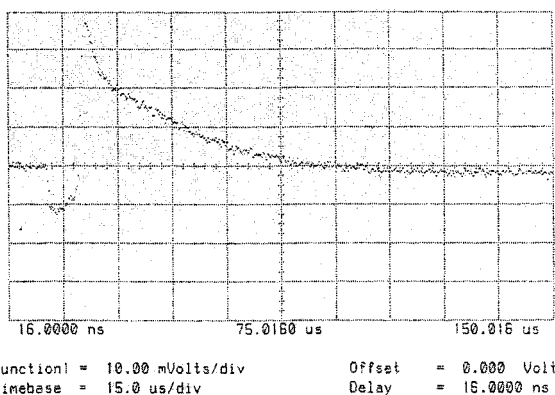
The measurement campaign fully confirmed all the theoretical considerations made in Section V. As cases (d) in Figs. 11–13 confirm, the waveforms given by (11) and by (4) are initially nearly identical. The two waveforms start to differ after the arrival of the echo generated by the first discontinuity along the loop, i.e., just when the role of the finiteness



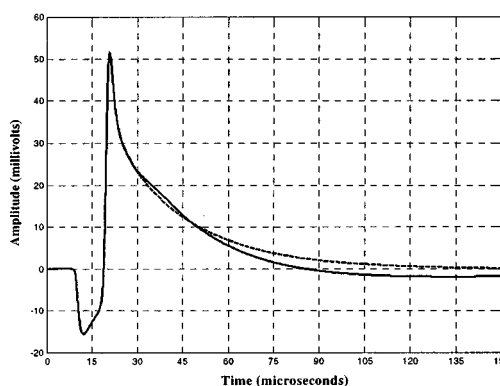
(a)



(b)



(c)



(d)

Fig. 13. Gauge Change: Comparison of measurement results and simulation results for the loop constituted of a 3-kft AWG 26 cable followed by 3 kft of a AWG 24 cable. Probing signal: 5-V and 1- μ s-square pulse.

of the loop comes into play and the boundary conditions have changed. Moreover, comparing the computer generated waveforms with the measured ones also confirmed the accuracy of our model for the computation of the primary characteristics of the twisted pair.

As mentioned in the Introduction, since signals have to travel a complete round trip when single-ended testing is considered it would appear that very high amplitude pulses and very sensitive equipment should be used in order to detect very weak echoes. However, it is worth pointing out that equipment today available on the market is sufficiently sensitive to allow us to detect echoes coming back from as far as 18 kft of AWG 24. As an example, in Fig. 14, we show the echo (after the subtraction of the slowly decaying signal) from an unterminated 18-kft AWG 24 loop obtained using only a 5-V probing pulse. When a 5-V pulse is used, the peak of the echo is around 9 mV. Since we expect that, in practice, it is possible to use pulses of 100 Vs or more, we expect that echo detection via TDR testing on loops up to 18 kft is indeed possible.⁵

At the beginning of Section II, we mentioned that the reflection coefficient $\rho(f)$ is different for each discontinuity and puts

⁵Loops over 18 kft must be loaded even when supporting simple voice services and, therefore, are not able to support DSL services. For this reason, only loops up to 18 kft are candidates for DSL services.

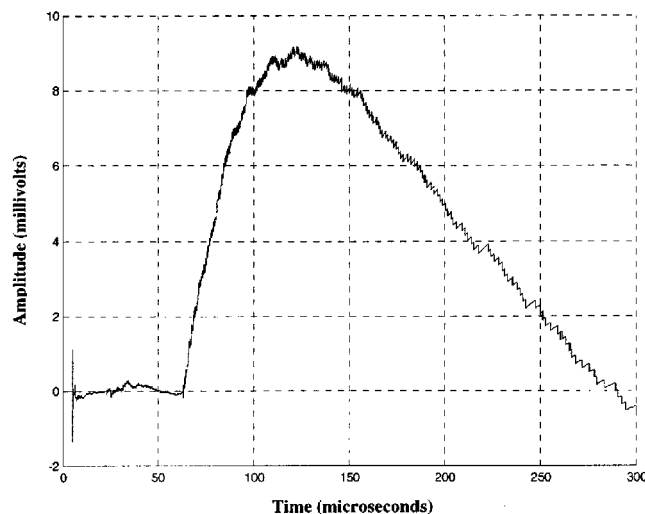


Fig. 14. Echo trace obtained subtracting the slowly decaying signal of (10) from a measured TDR trace. The loop is an unterminated 24-AWG gauge loop of 18498 ft. As predicted by theory, a positive echo indicating the end of the loop is present. Probing signal: 5-V and 5- μ s square pulse.

a sort of “discontinuity signature” on the echo. This can be seen looking at Fig. 15, where the echoes generated by four different discontinuities located at a distance of 9 kft from the CO are

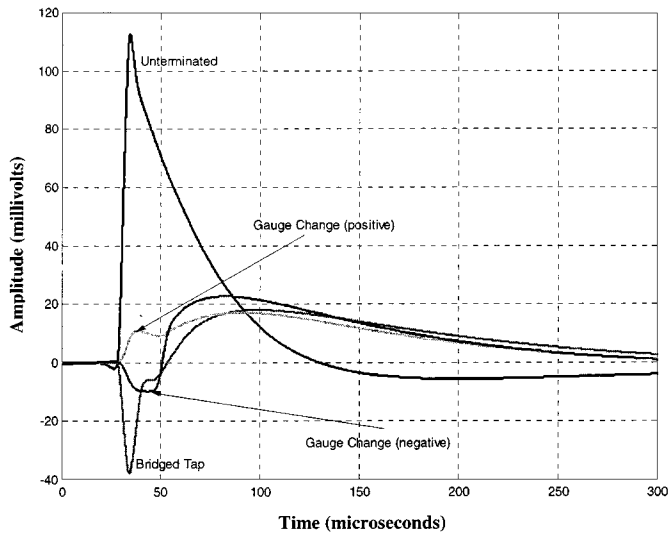


Fig. 15. Simulated echo traces representing the shape of the echoes generated by four different discontinuities located at a distance of 9 kft from the CO. Probing signal: 5-V and 5- μ s square pulse.

compared. 1) *End of Loop*: unterminated loop of 9 kft, AWG 24; 2) *Gauge Change (positive)*: 9 kft of AWG 24, followed by a 6 kft of AWG 26; 3) *Gauge Change (negative)*: 9 kft of AWG 24, followed by a 6 kft of AWG 22; 4) *Bridged Tap*: 9 kft of AWG 24, followed by a bridged tap of AWG 24 and 2 kft long, followed by another section of 6 kft of AWG 24. As the figure clearly shows, different discontinuities give rise to echoes of considerably different shape so that loop makeup identification can indeed be achieved via single-ended TDR techniques (see also [7]).

VII. CONCLUSION

In this paper, the problem of loop makeup identification by single-ended measurements is addressed. Identification of the loop makeup is sufficient to then qualify the loop for DSL service, an important emerging application in the telephone network. Moreover, the complete loop makeup can further be used to update records in loop databases, where records can in turn be accessed to support engineering, provisioning and maintenance operations. The proposed approach consists of probing the loop and waiting for the return of echoes generated by the discontinuities, i.e., a TDR-like approach. The underlying physical phenomenon that allows us to estimate the loop makeup is that gauge changes, bridged taps and the end of a loop represent a change in the characteristic impedance (a *discontinuity*) along the loop. When a signal is injected into a transmission-line, a reflected and a transmitted wave are generated corresponding to a change in the characteristic impedance. From the time of arrival of the echo, the location of the corresponding discontinuity can be easily estimated.

However, it has also been shown that today's conventional TDR technology is not capable of detecting all the echoes generated on a long loop. The major reason for these limitations is that conventional metallic TDRs do not take into account the distributed RLC nature of the loop and do not compensate for the

slowly decaying waveform that masks most of the weak echoes. The presence of this slowly decaying signal has not been reported in previous literature and is characterized here for the first time. The exact analytical expression of this slowly decaying signal has been given, and a technique to exploit this result has also been proposed. This technique consists of subtracting the slowly decaying signal from the available observations, thus allowing us to detect echoes that were previously masked. The subtraction of (10) from (9) is a very powerful technique that allows us to detect very far discontinuities. Moreover, this technique is also fundamental for the detection of gauge changes that would not otherwise be detectable.

A model that fully characterizes the echoes available at the CO has been derived and experimentally validated. On the basis of the derived model it has also been shown that the observations available at the receiver consist of an unknown number of echoes, some overlapping, some not, some spurious, some not, that exhibit unknown amplitude, unknown time of arrival and unknown shape. The resolution of such echoes via a single sensor is still an open mathematical problem and has been scarcely studied in the past literature. A novel approach to the solution of this problem will be proposed in [7].

ACKNOWLEDGMENT

The authors wish to thank J. Lamb, J. Dixon, and K. Kerpez for their insightful comments and their help in garnering the experimental data. A special thanks to T. Banwell, who was always available for stimulating discussions and was instrumental in allowing us to obtain very clean and precise measurements.

REFERENCES

- [1] *Transmission Systems for Communications*, Fifth ed: Bell Laboratories, 1982.
- [2] T. Starr, J. M. Cioffi, and P. J. Silverman, Eds., *Understanding Digital Subscriber Line Technology*. New York: Prentice Hall, 1999.
- [3] S. Galli, "Exact conditions for the symmetry of a loop," *IEEE Commun. Lett.*, vol. 4, pp. 307–309, Oct. 2000.
- [4] C. Davidson, Ed., *Transmission Lines for Communications*. New York: Wiley, 1978.
- [5] Y. Bresler and A. H. Delaney, "Resolution of overlapping echoes of unknown shape," in *Proc. ICASSP*, vol. 4, Glasgow, Scotland, 1989, pp. 2657–2660.
- [6] Z. He and L. Li, "An iterative approach to the resolution of overlapping echoes of unknown signal shape," in *Proc. IEEE Int. Symp. Circuit and Systems 1990*, 1990, pp. 1569–1572.
- [7] S. Galli, "Loop makeup identification via single ended testing: A maximum-likelihood approach," to be submitted.
- [8] The telcordia DSL spectral compatibility computer. Managed by Kenneth J. Kerpez. [Online]. Available: <http://net3.argreenhouse.com>
- [9] D. L. Waring, S. Galli, K. Kerpez, J. Lamb, and C. Valenti, "Analysis techniques for loop qualification and spectrum management," in *Proc. Int. Wire and Cable Symp. IWCS'00*, Atlantic City, NJ, Nov. 13–16, 2000.
- [10] C. Zeng, C. Aldana, A. Salvekar, and J. Cioffi, "Crosstalk identification in DSL systems," *IEEE J. Select. Areas Commun.*, vol. 19, pp. 1488–1496, Aug. 2001.
- [11] S. Galli, C. Valenti, and K. Kerpez, "A frequency-domain approach to crosstalk identification in xDSL systems," *IEEE J. Select. Areas Commun.*, vol. 19, pp. 1497–1506, Aug. 2001.



Stefano Galli (S'95–M'98) received the Masters degree (Laurea) and the Ph.D. (Dottorato di Ricerca) degree in electrical engineering from the University of Rome "La Sapienza," Rome, Italy, in 1994 and 1998, respectively.

After completing his Ph.D., he continued as a Teacher Assistant in Signal Theory at the Info-Com Department of the University of Rome. At the same time, he began to work as a consultant for Italian telecommunications companies. In October 1998, he joined Bellcore (now Telcordia Technologies, an

SAIC company), Morristown, NJ, as a Research Scientist in the Broadband Access and Premises Internetworking Department. He has coauthored over 40 papers in international journals and conferences. His main research efforts are devoted to automatic loop qualification for xDSL services, to crosstalk modeling, and to the analysis and performance assessment of wireless home networks and power line communications. His research interests also include detection and estimation, adaptive channel equalization, and personal wireless communications.



David L. Waring (M'88–SM'92) received the Bachelor of Science degree in electrical engineering from Drexel University, Philadelphia, PA, in 1977, and the Master of Science degree in electrical engineering from Georgia Institute of Technology, Atlanta, GA, in 1978.

He began his career at Bell Laboratories, , designing subscriber loop electronics. He moved to Bellcore, at its inception, in 1984, where he worked on early Metropolitan Area Network field trials and led teams that proposed requirements for HDSL and ADSL. He was Project Manager of several industry-leading interactive digital video trials. He currently leads research into "last mile" broadband local access and customer premises networks. He has also performed recent work on projects relating to critical infrastructure protection (CIP), and he manages a related NIST (National Institute of Standards and Technology) grant program.